2011 IEEE/RSJ International Conference on
Intelligent Robots and Systems
September 25-30, 2011. San Francisco, CA, USA

Multipoint Sliding Probe Methods for *In situ* Electrical Transport Property Characterization of Individual Nanostructures

Zheng Fan, *Student Member, IEEE*, Xinyong Tao, Xiaodong Li, and Lixin Dong, *Senior Member, IEEE*

Abstract*—Sliding probe methods are designed for the in situ electrical property characterization of individual one-dimensional (1D) nanostructures by eliminating the contact resistance between the fixed-end support and the specimen. The key to achieve a high resolution is to keep a constant resistance between the other end of the specimen contacting to the sliding probe. To achieve this objective, we have developed several important techniques including multipoint continuous sliding, flexible probes, and specimen-shape adapting based on nanorobotic manipulation inside a transmission electron microscope (TEM). With a copper-nanowire-tipped probe, we have shown that a flexible probe facilitates the contact force control. The adapting of the shape of a probe tip is significant for keeping a constant contact area between the probe and the specimen. This can be implemented by using a soft probe or a tip with a shape resembling the profile of the specimen. Here we show that by flowing copper from a nanotube probe against the specimen, it is possible to make a well adapted shape of the tip to the specimen after the copper cooled down. By avoiding stick-slip motion and controlling the contact force and area, it will be possible to keep a constant contact resistance between the sliding probe and the specimen, hence significantly improve the measurement resolution. Sliding probe methods are an in situ technique characterized by higher resolution and simplicity in setup as compared with conventional two- and four-terminal methods, respectively. Furthermore, it is superior for local property characterization, which is of particular interest for hetero-structured nanomaterials and defect detection.

***Index Terms* — Sliding probe methods, in situ nanotechnology, nanorobotic manipulation, individual nanostructures, electrical transport property**

I. Introduction

In situ electrical transport property characterization of individual nanostructures is of growing interest for accelerating the development of novel nanomaterials, correlating the transport properties to their atomic structures, and selecting proper building blocks for the electronic, sensing, actuation, electromechanical, or electrochemical systems [1-3]. Conventionally, two-terminal (Fig. 1(a)) [2, 4] and four-terminal (Fig. 1(b)) [1, 5-7] methods using either fixed electrodes or movable probes have been typically applied in such measurements.

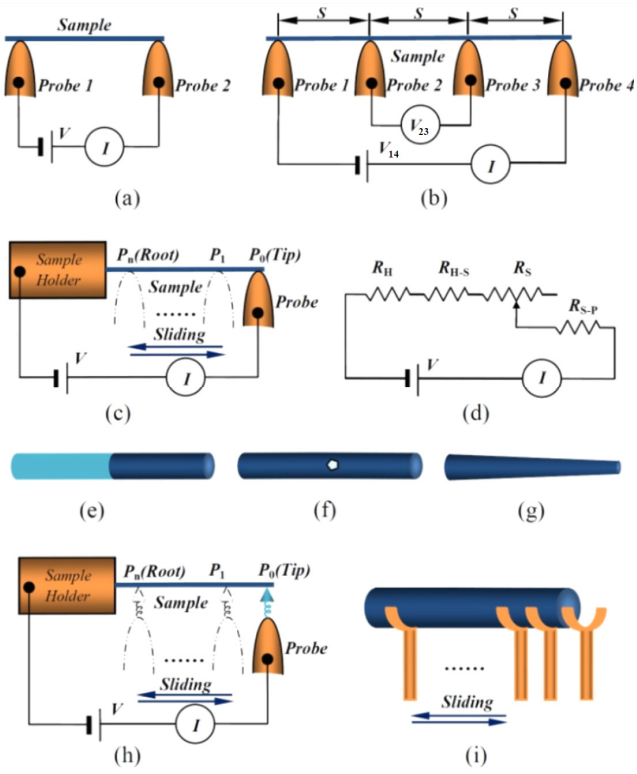

Fig.1 Schematic of electrical transport property characterization of an individual nanostructure. (a, b) Conventional two- and four-terminal methods. (c) Sliding probe methods for *in situ* electric property characterization. By contacting a probe to different points (P_0 (tip), P_1, …, P_n (root)) on an individual nanostructure, the resistance of the nanostructure is measured. (d) The equivalent circuit of the measurement loop, where R_H, R_{H-S}, R_S, and R_{S-P} represents the resistance of the sample holder, the contact resistance of the sample holder to the sample (a nanostructure), the resistance of the sample and the contact resistance of the probe to the sample, respectively. The method can be used to investigate a variety of nanostructures, particularly suitable for local transport measurement for a hetero-structure (e), a structure with local defects/doping (f), or a non-uniformed one (g). Enhanced techniques such as multipoint continuous sliding or differential ($n\rightarrow\infty$) sliding, together with flexible probes (h) and specimen shape-adapting (i) will broaden the application of the method and further improve its accuracy.

In theory, two-terminal methods (Fig. 1(a)) do not allow the determination of the intrinsic electrical transport properties due to the contact resistance between the probes and the sample that lies inside the measurement loop. The

Z. Fan and L. X. Dong are with the Department of Electrical and Computer Engineering, Michigan State University, East Lansing, MI 48824-1226, USA (phone: 517-353-3918; fax: 517-353-1980; e-mail: ldong@egr.msu.edu).

X. Y. Tao is with the College of Chemical Engineering and Materials Science, Zhejiang University of Technology, Hangzhou, Zhejiang 310014, China.

X. D. Li is with the Department of Mechanical Engineering, University of South Carolina, 300 Main Street, Columbia, SC 29208, USA.

Authorized licensed use limited to: Baylor University Libraries. Downloaded on May 31,2023 at 03:27:54 UTC from IEEE Xplore. Restrictions apply.

measurement accuracy is determined by the ratio of ($R_{P1\text{-}S}$ + $R_{S\text{-}P2}$)/R_S, where $R_{P1\text{-}S}$, $R_{S\text{-}P2}$, and R_S represents the contact resistance between the probes 1 and 2 and the nanostructure, and the intrinsic resistance of the nanostructure, respectively. Technically, it is possible to improve the contact by coating the probes with low-resistance materials, soldering the nanostructure onto the probes, or applying a compressing force using the probes to the nanostructure. Two-terminal methods have been applied in *in situ* characterization, especially for electromechanical coupling property characterization, due to its simplicity and agility when a manipulation probe is used. However, when the resistance of the nanostructure is close to the magnitude of the contact resistance, the conventional two-terminal method fails. A standard solution to eliminate the contribution of contacts is the four-terminal measurement. However, the application of this technique to an individual nanostructure is a challenge. Firstly, it is difficult to fabricate nanoelectrode or probe arrays with a nanoscale separation S (see Fig. 1(b)). The smallest separation to date is around 1μm. Secondly, it needs extra degrees of freedom for orientating the holder of the array to make contacts of the four probes to an individual nanostructure, which currently is hardly available from nanorobotic manipulators. Thirdly, it is particularly difficult to make four points to contact to a low-dimensional one such as a nanotube (NT) or a nanowire (NW), especially when they are free-standing. Finally, except for its high cost, it is a good solution to adapt four manipulators to position four separate probes onto a nanostructure. However, for the applications inside a transmission electron microscope (TEM), where the atomic resolution imaging of the nanostructure is achievable, this is not attainable due to the limitation of the specimen vacuum chamber.

Based on these insights, we have proposed a sliding probe method [8], in which a manipulation probe is used together with a fixed electrode or probe for the electrical property characterization (Fig. 1(c)). By contacting a probe to different local positions (e.g. the tip or the root) of an individual nanostructure, the resistance of the sample (nanostructure) can be measured by finding the difference between the two measurements.

II. Sliding Probe Methods

As shown in the equivalent circuit of the measurement loop (Fig. 1(d)), where R_H, $R_{H\text{-}S}$, R_S, and $R_{S\text{-}P}$ represent the resistance of the sample holder, the contact resistance of the sample holder to the sample, the resistance of the sample, and the contact resistance between the probe and the sample, respectively. The overall resistance when the probe contacts to any two points P_i and P_j (i, j = 0, 1, …, n and i < j) can be expressed as $R_i = R_H + R_{H\text{-}S} + R_{S,i} + R_{S\text{-}P,i}$ and $R_j = R_H + R_{H\text{-}S} + R_{S,j} + R_{S\text{-}P,j}$, respectively. So, the resistance of the sample between the points P_i and P_j is $R_{ij} = R_i - R_j = R_{S,i} - R_{S,j} + R_{S\text{-}P,i} - R_{S\text{-}P,j}$. It can be seen that the resistance of the sample holder and the contact resistance at the fixed end between the sample holder R_H and $R_{H\text{-}S}$ are eliminated. Hence, the difference between the two measurements when the probe contacts to any two points P_i and P_j of the nanostructure ($R_{ij} = R_i - R_j$) reflects the intrinsic resistance of the nanostructure between them ($R_{S,i} - R_{S,j}$) supposing that the contact resistance between the probe and the nanostructure are the same for the two cases ($R_{S\text{-}P,i} = R_{S\text{-}P,j}$). Compared with the conventional two-terminal method (Fig. 1(a)), only one side of the contact resistance is brought into the measurements. Hence, this sliding probe method holds higher accuracy for *in situ* electric property characterization whereas keeps simplicity as compared with 4-terminal methods. Furthermore, it is more feasible to keep the contact resistance between the probe and the sample at different positions to the same scale ($R_{S\text{-}P,i} \approx R_{S\text{-}P,j}$) than to eliminate the contact resistance ($R_{P1\text{-}S} \approx 0$ and $R_{S\text{-}P2} \approx 0$) at all as in the 2-terminal case.

Basic methods including two and three discreet points have been shown effective elsewhere [8] using nanorobotic manipulation inside a TEM. The method can be used to investigate a variety of nanostructures, particularly suitable for local transport measurement for a hetero-structure (Fig. 1(e)), a structure with local defects/doping sites (Fig. 1(f)), or a non-uniformly shaped one (Fig. 1(g)). In this report, we present several enhanced techniques for improving the uniformity of the contact resistance between the probe and the sample at different positions ($R_{S\text{-}P,i} \approx R_{S\text{-}P,j}$) and for broadening the applications of the method. These include (1) multipoint continuous sliding or differential ($n \to \infty$) sliding, (2) flexible probes (Fig. 1(h)), and (3) specimen-shape adapting of probe tips (Fig. 1(i)).

III. Experimental Setup

The experiments were performed in a TEM (JEOL 2200FS) with a field emission gun. The raw materials were attached to a 0.35 mm thick Au wire using silver paint, and the wire was held in the specimen holder. The probe was an etched 10 μm thick tungsten wire with a tip radius of approximately 100 nm (Picoprobe, T-4-10-1 mm). To improve the conductivity, the probes were coated with Au thin film (thickness: c.a. 21 nm). The motion control of the probe was carried out by an STM (scanning tunneling microscope)-TEM holder (FM2000E, Nanofactory Instruments AB). The probe can be positioned in a millimeter-scale workspace with a sub-nanometer resolution with the STM unit actuated by a three-degree-of-freedom piezotube, making it possible to select a specific object and fulfill the multi-point sliding probe measurement to different nanostructures.

IV. Multipoint Sliding Probe Measurements

Experiments are performed to demonstrate the electrical property measurement by applying the multipoint sliding probe method (Fig. 1(c)) to a variety of nano- and microstructures. The first demonstration is the IV characterization of an individual TaC nanowire. The second demonstration is the similar measurement applied to the carbon microfiber (CMF) where nanowires grow. The process of these measurements are as follows: to the individual nanowire, the STM probe respectively makes contact with two positions on the sample (Fig. 2(a)), including the tip (Inset: left) and the root (Inset: right) of the

Authorized licensed use limited to: Baylor University Libraries. Downloaded on May 31,2023 at 03:27:54 UTC from IEEE Xplore. Restrictions apply.

nanowire in two measurements. A bias was applied between the sample holder and the probe that swept from -500 mV to 500 mV. The current-voltage (IV) curves were taken simultaneously during this process. In regard to the carbon microfiber, the contacts were made on three positions on the sample by using the STM probe, including the tip (Inset: left), the middle (Inset: middle), and the root (Inset: right) of the nanowire in three measurements.

According to the IV properties, the resistance of carbide nanowires and carbon microfibers was changing in accordance with the current value. Therefore, a mathematical method was proposed to understand the resistance between the two contact areas. Firstly, to the measurement of TaC nanowire, we assume that the IV curves of TaC nanowire in tip and root (see Fig. 2(b)) are linearly fitted by:

$$I_C = aV_C + b \tag{1}$$

where, I_C is the current under the bias of V_C when the probe is on the contact area. Therefore, the resistance from the sample holder to the contact area is easy to be obtained. As we got the relation between the resistance and the current, the resistant between two contact areas can be derived as:

$$\begin{aligned} R_{ij} &= R_i - R_j = R_{S,i} - R_{S,j} + R_{S\text{-}P,i} - R_{S\text{-}P,j} \\ &= \frac{1-d/I_i}{c} - \frac{1-b/I_i}{a} + R_{S\text{-}P,i} - R_{S\text{-}P,j} \end{aligned} \tag{2}$$

Assuming that the contact resistances between the probe and the nanostructure are the same in the two contact areas ($R_{S\text{-}P,i} = R_{S\text{-}P,j}$). Therefore, the influence of contact resistance between the two areas was eliminated in equation (2). The fitted curve on the tip and root is: I_{Root}=0.6995V_{Root}-2.6529, the appropriateness of fitting here is X^2=0.9999; and I_{Tip}=0.6564V_{Tip}-2.5418, X^2=1.000, where I and V are in μA and mV, respectively (Fig. 2(b) and (c)). According to equation (2), as the influence of the contact resistance was erased, the resistance between the tip and root is 93.9 Ω (bias: -500 mV to -100 mV and 100 mV to 500 mV) in average. The diameter and the length of the nanowire are 292.0 nm and 10.0 μm, respectively, so the resistivity of the nanowire is calculated to be 63.6 μΩ·cm (bias: -500mV to -100mV and 100mV to 500mV) in average, which is comparable to the resistivity of bulk TaC materials [9] (137 μm thick and 4.6 cm long: 32.7-117.4 μΩ·cm for a variety of compositions). The measured value is closer to the average of two limits. The result reveals the accuracy of the measurement.

Secondly, to the measurement of CMFs (Fig. 3(a)), where the measured IV curves in these three positions can be perfectly fitted into a three degree polynomial (see Fig. 3(b)):

$$I_c = aV_c^3 + b\,V_c^2 + cV_c + d \tag{3}$$

To find an analytical solution to the above equation, we transform the equation into:

$$(aI_c^2)R_c^3 + (bI_c)R_c^2 + cR_c + (d/I_c - 1) = 0 \tag{4}$$

The resistance R_c from the sample holder to different contact areas can be solved from equation (4). Then, the

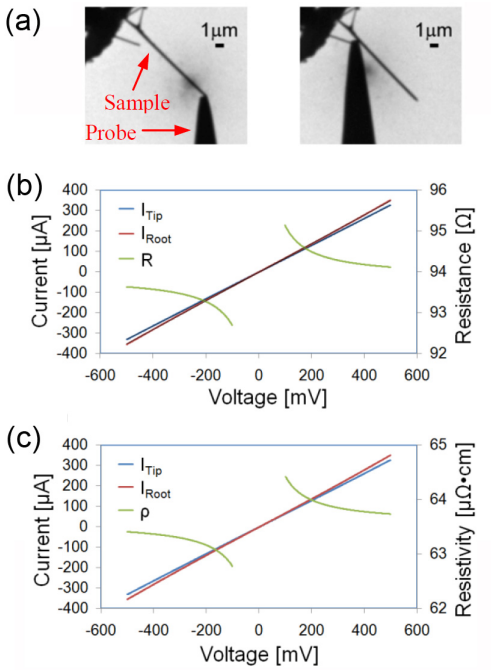

Fig. 2 Sliding probe technique for in situ electric property characterization of the TaC nanowire and the carbon microfiber. (a) The corresponding TEM image for the TaC nanowire sliding probe characterization. A STM probe contacts to the tip (left) and the root (right) of the nanowire in two measurements, respectively. (b) IV characterization and the resistance curve of a TaC nanowire using the sliding probe method. A bias is applied between the sample holder and the probe and swept from -500 mV to 500 mV. The resistance is found from the slope of the linear IV curves. The resistance here is calculated to be 93.9Ω (bias: -500mV to -100mV and 100mV to 500mV) in average. (c) IV characterization and the resistivity curve of a TaC nanowire using the sliding probe method. As the diameter of the nanowire is 290.2nm and the length of it is 9.8μm, the resistivity of it is calculated to be 63.6±0.8 μΩ·cm (bias: -500mV to -100mV and 100mV to 500mV) in average.

resistance between these contact areas can be calculated using equation (2). The fitting curves on tip, middle and root are shown as follows:

$$I_{Tip} = 5.0\times10^{-5}V_{Tip}^3 - 5\times10^{-4}\,V_{Tip}^2 + 24.541V_{Tip} - 190.96 \quad X^2 = 0.9997 \tag{5}$$

$$I_{Mid} = 4.0\times10^{-5}V_{Mid}^3 - 1.8\times10^{-3}\,V_{Mid}^2 + 33.111V_{Mid} - 127.46 \quad X^2 = 0.9999 \tag{6}$$

$$I_{Root} = 2.0\times10^{-5}V_{Root}^3 - 1.0\times10^{-4}\,V_{Root}^2 + 41.76V_{Root} - 193.3 \quad X^2 = 1.0000 \tag{7}$$

where, I_{Tip} is the current under the bias of V_{Tip} when the probe contacts on the tip; I_{Mid} is the current under the bias of V_{Mid} when the probe contacts on the middle; I_{Root} is the current under the bias of V_{Root} when the probe contacts on the root. V_{Root}, V_{Mid} and V_{Tip} here are the biases which swept from -500 mV to 500 mV when the probe contacts the carbon microfiber in three positions.

According to equation (2), the resistance of it was calculated to be 32.3 kΩ from tip to mid and 11.1 kΩ from mid to root (bias: -500 to -100 mV and 100 to 500 mV) in average. The average diameter and the length of the carbon fiber from tip to mid are 2.2 μm and 29.7 μm, and from mid to root are 2.2 μm and 23.8 μm, respectively. As a result, its resistivity was calculated to be 0.2-0.7 Ω·cm and 0.1-0.2

Authorized licensed use limited to: Baylor University Libraries. Downloaded on May 31,2023 at 03:27:54 UTC from IEEE Xplore. Restrictions apply.

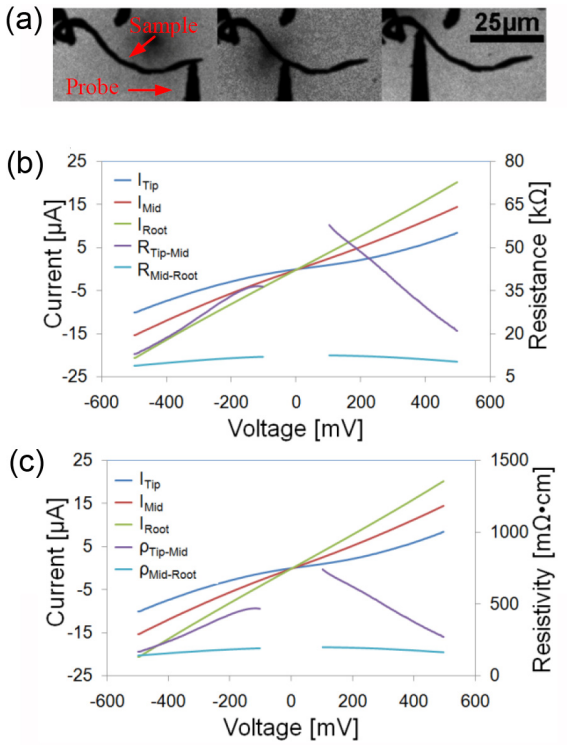

Fig. 3 Sliding probe technique for in situ electric property characterization of a carbon microfiber. (a) The corresponding TEM image for the sliding probe characterization of carbon microfiber. A STM probe contacts to the tip (left), center (mid) and the root (right) of the microfiber with three measurements taken, respectively. (b) IV characterization and the resistance curve of the carbon fiber. A bias is applied between the sample holder and the probe and swept from -500 mV to 500 mV. The resistance is found from the slope of the linear IV curves. The resistance here is calculated to be 32.3kΩ from tip to mid and 11.1kΩ from mid to root (bias: -500mV to -100mV and 100mV to 500mV) in average. (c) IV characterization and the resistivity curve of the carbon fiber. The diameter of the carbon fiber from tip to mid is 297.6nm and the length of it is 29.7μm.The diameter from mid to root is 297.6 nm and the length is 23.8 μm. The resistivity of it is calculated to be 0.2-0.7 Ω·cm and 0.1-0.2 Ω·cm (bias: -500mV to -100 mV and 100mV to 500mV) respectively.

Ω·cm (see Fig. 3(c)). The fact that the resistivity of these two parts is very close indicates the accuracy of the sliding method.

The result of multipoint sliding probe method precisely reveals the electrical properties of nanostructures. The results show the high conductivity of the carbide NWs. To the TaC NWs, the resistivity is 63.6 ± 0.8μΩ·cm. According to our sliding probe measurements of the CMF from which NbC NWs growed, the resistivity is within the range of 0.1-0.7 Ω·cm.

V. Flexible Probe Differential Sliding Measurements

Based on multipoint sliding, a high accuracy in the transport property characterization can be achieved by fully removing the contact resistance on the fixed end and partially erasing that on the sliding side. To further improve the measurement resolution, the contact force and area between the probe and the sample will need to be controlled to keep a constant contact resistance. To keep a constant force, an elastic contact will be preferred compared to a stiff

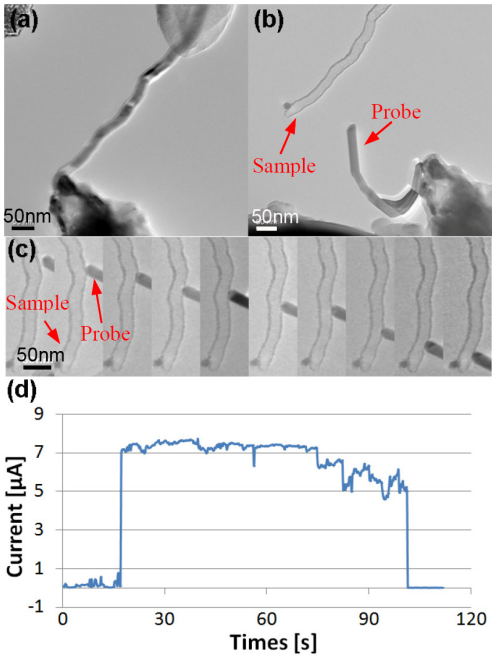

Fig. 4 (a) The copper-filled CNT and the probe; (b) Soft probe fabrication. By using the EMBD, a copper stick is deposited on the tip of probe, and the stick is served as a new probe to acquire more accuracy. (c) The differential sliding to a single CNT, the probe sliding on a copper filled carbon nanotube in a uniformed speed (about 10nm/s) under the bias of 500mV, the resistance of it along the moving direction is found during the sliding process. (d) The IT curve recorded by differential sliding method. During the sliding, the current value steadily decreased along the length of CNT, described precisely about the increasing of resistance.

one. To keep a constant area, shape adaptable probe tip is superior to a point tip due to the readiness to keep the contact and the average effect over the contact area.

As a result, a flexible probe sliding measurement is proposed in this section for the first objective, which is particularly suitable to the measurement of non-uniformed nanostructures, such as an irregularly shaped CNT (Fig. 4). A copper nanowire was fabricated on the tungsten probe tip by using the electromigration-based deposition (EMBD) [10] (Fig. 4(a) and (b)). The physical contacts were made between the copper nanowire and the sidewall of a nanotube for the measurement.

The copper nanowire serves as a flexible probe. It is prepared by applying a voltage between the tungsten probe and the sample holder, which establishes an electrical circuit through a copper-filled CNT and injects thermal energy into the system via Joule heating. By increasing the applied voltage, the local temperature can be increased past the melting point of the copper encapsulated inside a tube. Then, the encapsulated materials can be delivered from the carbon shells. Hence, a nanoscale soft probe was fabricated on the tip of the original tungsten probe.

It is noted that the attractive surface force largely depends on the volume of the contact objects. As the volume of the nanoscale flexible probe is much smaller than the STM probe (tip radius: 100 nm, root radius: 10 μm), the surface force induced binding between the sample and the probe during sliding will be decreased. Hence, it is easier to keep a constant contact force by using the nanoscale flexible

Authorized licensed use limited to: Baylor University Libraries. Downloaded on May 31,2023 at 03:27:54 UTC from IEEE Xplore. Restrictions apply.

probe. Furthermore, in previous investigations, either using a fixed electrode or a movable probe, the contact has been made only on several positions on a sample. The limited number of contact points can provide data to describe the general characteristics of the nanostructure but not local properties, hence, a differential sliding technical is proposed to combine the application of the soft probe. When the soft probe continuously slides on a copper-filled carbon nanotube at a uniform speed (about 10nm/s) under a bias of 500mV (Fig. 4(c)), the resistance along the moving direction was measured simultaneously. The current value steadily decreased along the length of CNT, while the resistance increased (Fig. 4(d)).

This differential sliding method using a soft probe has the advantage that the change of the contact resistance R_c can be neglected during the measurement. Furthermore, the stick-slip effect can be largely erased with soft probe sliding. Based on the current-time (I-t) curve and a real time video based on the TEM obtained during the sliding process, the sliding speed, the bias between the probe and CNT, and the resistance versus length curves can be obtained.

In the experiment, the original data fit a straight line with the appropriateness of X^2=0.8211, however, if the resistivity of the CNT is a constant, the increase of resistivity will match the increased length of the CNT closer. It means that the resistance-length (RL) curve should fit more closely to a one-order equation.

It has been found that the measured resistance is affected by the impact of the probe during the sliding (Fig. 5(a)). In order to reveal the relation between the impact force ΔF and the resistance ΔR that affected by it, we correlate them with:

$$\Delta R=\sigma \bullet \Delta F \tag{8}$$

and

$$\Delta F=3\Delta EI/L^3 \tag{9}$$

where, ΔE is the deformation of the CNT, I is the moment of inertia of the CNT, and L is the length of CNT.

Then, the relation between ΔR and ΔE can be given by:

$$\Delta R=\delta \bullet \Delta E \tag{10}$$

In order to obtain the parameter δ, the probe purely impacted the CNT without sliding movement during this process is considered. The influence by the sliding of CNT can then be eliminated. The current value is taken simultaneously during this approach. Therefore, the impacted electrical variety can be recorded. Before the impact, the distance between the tip of the CNT and the reference line before the impact is 5.14 nm (see Fig. 5(a)). After the impact, the distance increased to 8.82 nm. The deformation is calculated to be 3.68 nm. The correspondent impact force is 187.8 pN, and the resistance change during this approach is 0.95 kΩ. The parameter δ was calculated to be 5.07 Ω/pN.

As a result, the resistance of the CNT after eliminating the influence of the impact R_{ei} can be presented as $R_{ei}=R-\Delta R$. The appropriateness of the one-order fitted curve reached 0.9376 (Fig. 5(b)), which is a significant improvement to the previous approach. The fitted one-order equation here is given by:

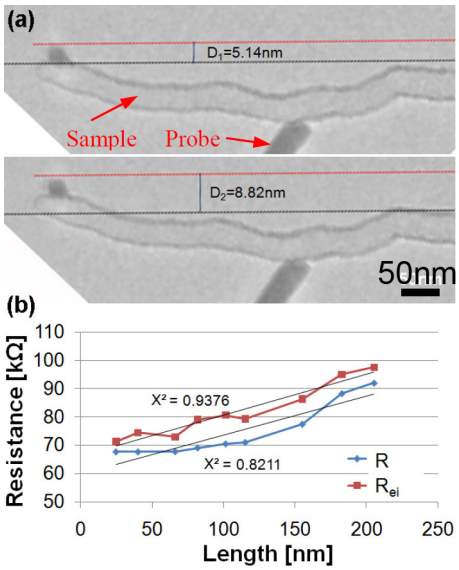

Fig. 5 The impacting test of a CNT. (a) The blue line is a reference line to the CNT, and the red line shows the top position of it. The distance between the tip of the CNT and the reference line before the impact is 5.14nm. After the impact, the distance increased to 8.82nm. Therefore, the deformation here is 3.68nm, and the correspondent impact force is 187.8pN. According to the change of resistance during this approach is 0.95kΩ, then the parameter δ is calculated as 5.07 Ω/pN. (b) The resistance versus length curve during the sliding process. The RL curve represents the resistance before the elimination of the impact force influence versus the length of CNT, which can be fitted by a one-order curve with the appropriateness of 0.8211. After the elimination of the impact force influence, the correspondent R_{ei}L curve has an improved fitted appropriateness of 0.9376.

$$R_{ei} = 0.1449L + 66.162 \tag{11}$$

Moreover, the equation for the resistivity of a single conductor is shown as:

$$\rho = R/L \bullet A \tag{12}$$

The differential sliding process consists of continuous/countless sliding steps. Each sliding step represents a single measurement to the nanostructure. Therefore, the resistivity of single measurement is:

$$\rho_i = \Delta R_i/\Delta L_i \bullet A_i \tag{13}$$

The resistance increased simultaneously when the probe was sliding along the CNT. The curve was fitted with a one-order curve. Therefore, the $\Delta R/\Delta L$ here is the same in each measurement, which can be expressed as a differential formula $dR(L)/dL$. As a result, the average resistivity ρ' can be derived as:

$$\rho' = dR(L)/dL \bullet A' \tag{14}$$

where, A' is the average cross section area of the CNT. The area equals to 390 nm^2. From equation (14), $dR(L)/dL$ is calculated to be 0.1449 kΩ/nm. The average resistivity is then obtained as 5.65×10^{-5}Ω·m. This value is comparable to the four point measurements of a supported, unfilled multi-walled carbon nanotube, where the resistivity was about 1×10^{-5}Ω·m with the cross section area about 200-314 nm^2 [11].

Authorized licensed use limited to: Baylor University Libraries. Downloaded on May 31,2023 at 03:27:54 UTC from IEEE Xplore. Restrictions apply.

VI. Adapted Probe Measurements

The attempt to measure the non-uniformed nanostructure by using soft probe differential sliding method was a good approach with high accuracy and simplicity; however, to the nanostructure with local defects or hetero-structured, the soft probe method may not precisely reveal the electrical property of the nanostructure. Due to the changing of contact area during the soft probe sliding, the contact resistance was variable, which means that the measured electrical property was influenced also.

As a result, a shape adapted probe sliding method was proposed. The adapting of the shape of a probe tip is significant for keeping a constant contact area between the probe and the specimen. Here we show that by using the same method as in the soft probe fabrication, the copper inside the CNT would flow out from a nanotube against the specimen (see Fig. 6(a) and (b)). It is possible to reheat and reshape a deposited copper which is not close to the probe [10] by repeatedly attaching the CNT to the copper stick. After then, a perfectly adapted shape of the tip to the specimen would be possible to fabricate after the copper cooled down (Fig. 6(c)).

The adapted probe sliding method is a new approach for the electrical transport characterization of irregular shaped nanostructures. With the combination of the adapted probe tip and the soft probe differential sliding method, the stick-slip motion can be avoided and the contact force and area can be controlled (Fig. 6(d)). This approach will be possible to keep a constant contact resistance between the sliding probe and the specimen, hence significantly improve the measurement resolution. The feasibility and the accuracy of this method enable us to explore the detail of electrical properties of one single nanostructure in a high efficient mode.

VII. Conclusions

To characterize the transport properties of individual nanostructures, we have developed several enhanced *in situ* techniques for multipoint sliding methods including multipoint continuous sliding, flexible probes, and specimen-shape adapting based on nanorobotic manipulation inside a TEM. With a copper-nanowire-tipped probe, we have shown that a flexible probe facilitates the contact force control. The adapting of the shape of a probe tip is significant for keeping a constant contact area between the probe and the specimen. This has been implemented by using a copper tip with a shape resembling the profile of the specimen. The tip was prepared by flowing copper from a copper-filled nanotube against the specimen. By controlling the contact force and area, it became possible to keep a constant contact resistance between the sliding probe and the specimen, hence significantly improved the measurement resolution. Sliding probe methods are an in situ technique characterized by higher resolution and simplicity in setup as compared with conventional two- and four-terminal methods, respectively. Furthermore, it is superior for local property characterization, which is of particular interest for hetero-structured nanomaterials and defect detection.

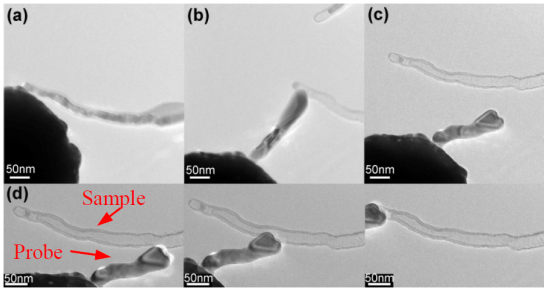

Fig. 6 (a) The copper-filled CNT and the probe; (b) The inner copper flowed out from the CNT; (c) Shape adapted probe fabrication: By repeatedly attaching the CNT to the copper stick, the deposited copper tip would be reheated and reshaped to a perfectly adapted shape of the tip to the specimen; (d) The shape adapted sliding process, which may improve the accuracy by keeping a constant contact resistance. (Scale bars: 50 nm)

Acknowledgement

This work is supported by the NSF (IIS-1054585), the NSFC (51002138), the Zhejiang Provincial NSF of China (Y4090420), the NSF (CMMI-0968843, CMMI-0824728, CMMI-0653651), the Qianjiang Talent Project (2010R10029), the 'Qianjiang Scholars' program and the project sponsored by the Project sponsored by SRF for ROCS (2010609), SEM.

References

[1] T. W. Ebbesen, H. J. Lezec, H. Hiura, J. W. Bennett, H. F. Ghaemi, and T. Thio, "Electrical conductivity of individual carbon nanotubes," *Nature,* vol. 382, no. 6586, pp. 54-56, Jul. 1996.

[2] H. J. Dai, E. W. Wong, and C. M. Lieber, "Probing electrical transport in nanomaterials: Conductivity of individual carbon nanotubes," *Science,* vol. 272, no. 5261, pp. 523-526, Apr. 1996.

[3] L. X. Dong, A. Subramanian, and B. J. Nelson, "Carbon nanotubes for nanorobotics," *Nano Today,* vol. 2, no. 6, pp. 12-21, Dec. 2007.

[4] S. J. Tans, M. H. Devoret, H. J. Dai, A. Thess, R. E. Smalley, L. J. Geerligs, and C. Dekker, "Individual single-wall carbon nanotubes as quantum wires," *Nature,* vol. 386, no. 6624, pp. 474-477, Apr. 1997.

[5] B. Gao, Y. F. Chen, M. S. Fuhrer, D. C. Glattli, and A. Bachtold, "Four-point resistance of individual single-wall carbon nanotubes," *Physical Review Letters,* vol. 95, no. 19, art. no. 196802, Nov. 2005.

[6] S. Yoshimoto, Y. Murata, K. Kubo, K. Tomita, K. Motoyoshi, T. Kimura, H. Okino, R. Hobara, I. Matsuda, S. Honda, M. Katayama, and S. Hasegawa, "Four-point probe resistance measurements using Ptlr-coated carbon nanotube tips," *Nano Letters,* vol. 7, no. 4, pp. 956-959, Apr. 2007.

[7] R. Lin, M. Bammerlin, O. Hansen, R. R. Schlittler, and P. Boggild, "Micro-four-point-probe characterization of nanowires fabricated using the nanostencil technique," *Nanotechnology,* vol. 15, no. 9, pp. 1363-1367, Sep. 2004.

[8] Z. Fan, X. Y. Tao, Y. P. Li, Y. C. Yang, J. G. Du, W. K. Zhang, H. Huang, Y. P. Gan, X. D. Li, and L. X. Dong, "In situ electrical property characterization of individual nanostructures using a sliding probe inside a transmission electron microscope," in *Proc. of the 2010 IEEE Nanotechnology Materials and Devices Conference (IEEE-NMDC2010)*, Monterey, California, Oct. 12-15, 2010, pp. 149-152.

[9] J. R. Cooper and R. L. Hansler, "Variation of electrical resistivity of cubic tantalum carbide with composition," *Journal of Chemical Physics,* vol. 39, no. 1, pp. 248-249, 1963.

[10] Z. Fan, X. Y. Tao, X. D. Cui, X. D. Fan, X. B. Zhang, and L. X. Dong, "Shaping the nanostructures from electromigration-based deposition," in *Proc. of the 2010 IEEE Nanotechnology Materials and Devices Conference (IEEE-NMDC2010)*, Monterey, California, Oct. 12-15, 2010, pp. 22-25.

[11] C. Schonenberger, A. Bachtold, C. Strunk, J. P. Salvetat, and L. Forro, "Interference and interaction in multi-wall carbon nanotubes," *Applied Physics A-Materials Science & Processing,* vol. 69, no. 3, pp. 283-295, 1999.

Authorized licensed use limited to: Baylor University Libraries. Downloaded on May 31,2023 at 03:27:54 UTC from IEEE Xplore. Restrictions apply.